ELSEVIER

Journal of Alloys and Compounds 401 (2005) 165–172

Journal of ALLOYS AND COMPOUNDS

www.elsevier.com/locate/jallcom

Investigation of Gd compounds using synchrotron radiation

B. Tyszka [a], J. Szade [a,*], W. Burian [a], G. Skorek [a], J. Deniszczyk [b], M. Sikora [c], D. Zając [c], Cz. Kapusta [c], M. Matteucci [d], F. Bondino [d], M. Zacchigna [d], M. Zangrando [d]

[a] *A. Chelkowski Institute of Physics, University of Silesia, Uniwersytecka 4, 40-007 Katowice, Poland*
[b] *Institute of Physics and Chemistry of Metals, University of Silesia, Uniwersytecka 4, 40-007 Katowice, Poland*
[c] *AGH University of Science and Technology, Mickiewicz Avenue 30, 30-059 Krakow, Poland*
[d] *INFM-TASC, Beamline BACH, AREA Science Park, 34012 Basovizza, Trieste, Italy*

Received 28 July 2004; received in revised form 25 November 2004; accepted 1 December 2004
Available online 27 June 2005

Abstract

The electronic structure of ferromagnetic compound GdTiGe has been investigated using element sensitive methods—X-ray absorption spectroscopy (XAS), X-ray magnetic circular dichroism (XMCD) and resonant inelastic X-ray scattering (RIXS). Additionally, another ferromagnet GdTiSi has been studied using XMCD. XMCD revealed a strong dichroic signal at Gd L_2 and L_3 edges, which can be related to polarisation of Gd 5d band. XAS at Ti $L_{2,3}$ edges has exhibited a structure which appeared to be in general agreement with the LAPW calculations. RIXS spectra have shown some resonance features for photon energies close to Ti L_2 and Gd M_5 edges.

Keywords: Intermetallics; X-ray spectroscopies; Synchrotron radiation; Gadolinium titanium germanate; Gadolinium titanium silicate

1. Introduction

The group of GdTX compounds, where T is a transition 3d element and X is Ge or Si, has been widely investigated mainly due to a variety of interesting magnetic and electronic properties. Only a few compounds with titanium have been found to exist. We reported on ferromagnetism in GdTiGe with a high $T_C = 374$ K [1]. It exhibits the highest Curie temperature within the group of rare earth compounds with non-magnetic elements. The analysis of the powder X-ray diffractograms shows that GdTiGe crystallizes in a tetragonal CeScSi type of structure (space group *I*4/*mmm*). For GdTiGe, the lattice constants are $a = b = 0.4079(1)$ nm, $c = 1.545(5)$ nm. GdTiSi crystallizes in a tetragonal CeFeSi type of structure (*P*4/*nmm*). It exhibits also ferromagnetic type of ordering with high Curie temperature (294 K). The magnetisation below T_C for GdTiSi is however much smaller than for GdTiGe [1].

The aim of this work is to study the detailed electronic structure of GdTiGe and partly of GdTiSi in order to understand the peculiar properties. Earlier photoemission data of the valence band have been compared to the calculations using the TB LMTO method and a reasonable agreement has been obtained [1].

The element specific magnetic electronic structure of these compounds is investigated with X-ray absorption spectroscopy (XAS) and X-ray magnetic circular dichroism (XMCD) measurements in the Ti, Ge and Gd core absorption regions. Additionally, the element specific excitations have been studied for GdTiGe using resonant inelastic X-ray scattering (RIXS). This technique has not been used so far for rare earth intermetallics. The experimental results are discussed in relation to the electronic structure calculations obtained within the TB LMTO and LAPW methods. This allows checking how the solid-state effects influence the spectra, which are usually analysed in an atomic approximation.

* Corresponding author. Tel.: +48 32 3591928; fax: +48 32 2588431.
E-mail address: szade@us.edu.pl (J. Szade).

0925-8388/$ – see front matter © 2005 Elsevier B.V. All rights reserved.
doi:10.1016/j.jallcom.2004.12.148

2. Experimental

GdTiGe and GdTiSi were obtained by the Czochralski method from a levitated melt. Gd of 99.9% purity, Ti 99.99%, Ge(Si) 99.999%. The melting point of investigated compound has been found to be very high and was estimated to be close to 2000 K. The sample consisted of large grains. One of the disk shaped grains has been used for XAS and RIXS investigations (about 2 mm diameter).

The resonant emission spectra were acquired with the ComIXS fluorescence spectrometer at the Beamline for Advanced Dichroism (BACH) of ELETTRA (Trieste, Italy). The spectrometer, based on an innovative optical design, is equipped with a detector consisting of a CCD camera with 20 μm × 20 μm pixels, and two variable line spacing spherical gratings. The spectrometer exploits the small spot size, high flux and controllable polarisation of BACH station. The sample surface was perpendicular to the beam and made an angle of 60° with the X-ray emission analyzer.

The XAS spectra at ELETTRA were measured by means of total electron yield by direct detection of the sample photocurrent and changing the photon energy. The incident photon energies were calibrated using the elastic peak measured in the X-ray emission spectra. Unfortunately, the XMCD measurements at the BACH beamline were performed at room temperature and no dichroism was observed.

Moreover XAS measurements at the Ge K-edge, as well as at the Gd L_2 and L_3 edges have been carried out at the bending magnet beamline A1 of the Hasylab/DESY in Hamburg. The spectra were recorded at 5 K for polycrystalline powder samples of GdTiGe and GdTiSi using transmision mode in an applied magnetic field of 1 T, flipped at each energy. The degree of circular polarisation behind double crystal Si(1 1 1) monochromator was estimated to $P_C = 75\%$, 68% and 67% for Ge K, Gd L_2 and Gd L_3 edge, respectively, with a resolving power of $E/\Delta E \sim 10^4$. For the studies at the Ti K-edge the resolving power was about 5×10^3 and P_C was about 35–40%. All spectra have been measured four times, twice for each sequence of magnetic field flipping (NSSN, SNNS) in order to minimize systematic errors. XAS spectra corresponding to the XANES range were carefully background subtracted and normalized to the edge step. X-MCD spectra obtained by subtraction of the XANES spectra measured for the magnetic field direction parallel and antiparallel to the beam were normalized to the degree of circular polarisation of X-rays.

3. Results and discussion

In a simplified view, X-ray absorption spectroscopy probes empty levels above the Fermi energy. An electron is promoted from a core state to some state at (or just above) the Fermi energy and a filled state from just below the Fermi level recombines with the core hole emitting a scattered photon. In the XAS spectra of 3d transition metals, two transitions

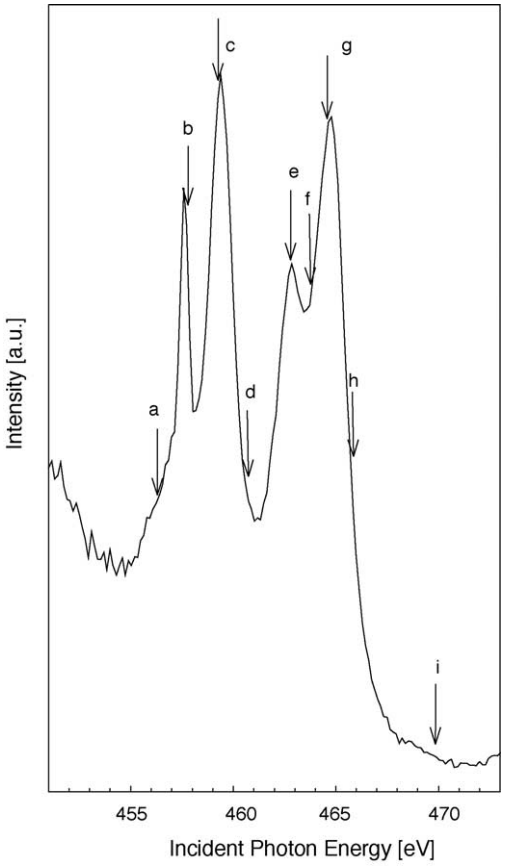

Fig. 1. Ti $L_{2,3}$-edge XAS spectrum of GdTiGe.

are the most important [2]: the dipole allowed 2p–3d and the quadrupole allowed 3d–3d. These two particle interactions split the XAS final state into a large number of atomic multiplets. Our spectrum of Ti L_2 and L_3 edges shows a well developed structure (Fig. 1) which can be compared to the existing calculations and results from other Ti compounds. Atomic multiplet splitting calculations include: spin–orbit coupling of the 2p hole (which causes the division of the 2p edge into the L_3 and L_2), 2p–3d Coulomb and the exchange interaction. In order to simulate the solid crystal we also need an extra term, which will describe the cubic crystal field effect on the $3d^n$–$2p^5 3d^{n+1}$ excitation. De Groot and Fuggle [3] calculated multiplet spectrum for the $3d^0$–$2p^5 3d^1$ excitations of Ti^{4+} in octahedral symmetry, which is similar to our experimental XAS spectrum (Fig. 1). The splitting between the two main peaks within both the L_3 and L_2 edges is related to the crystal-field splitting.

The experimental data obtained for oxide compounds containing Ti show the structure, which is in agreement with the calculations of de Groot and Fuggle [3]. Recent work by Stener and Fronzoni [4] gives different Ti 2p absorption structure in $TiCl_4$ in both experimental and theoretical studies. However, to our knowledge, there is no data on metallic Ti compounds. For such materials the solid-state effects, such as band structure should be taken into account

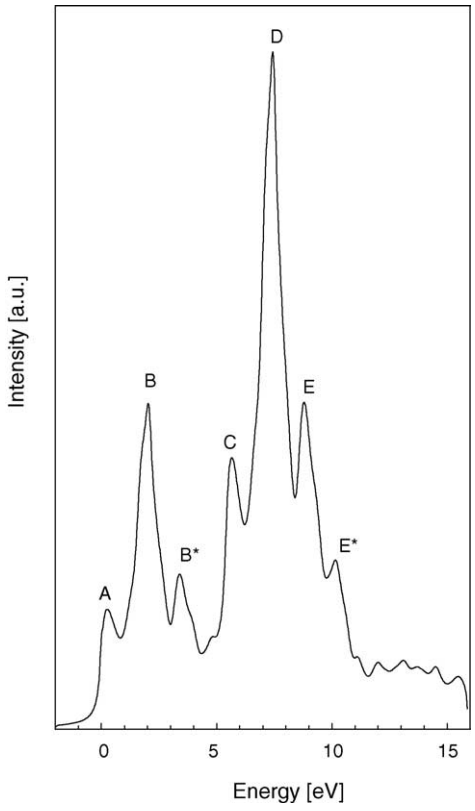

Fig. 2. Calculated Ti $L_{2,3}$-edge XAS spectrum of GdTiGe.

when modelling absorption spectra. The Ti $L_{2,3}$ XAS model spectrum in GdTiGe (Fig. 2) has been obtained with the LAPW method investigated by the general potential Linear augmented plane wave (FP-LAPW) method, using the WIEN2k code of Blaha et al. [5].

In the FP-LAPW approach no shape approximation for the crystal potential was used. Within the muffin-tin (MT) atomic spheres, the potential and charge density were expanded into lattice harmonics up to sixth order. Outside the MT spheres, the plain wave expansion up to the reciprocal lattice vector of magnitude of $|\mathbf{G}_{max}| = 15$ was applied (3557 plane waves). The lattice parameters were taken from experiment [1]. In the calculations the same radius (2.6 a.u.) was assumed for all MT atomic spheres, which fills roughly the half of the unit cell volume.

In the all-electron calculations, the following electronic configurations were assumed: for Gd the (Xe) $4f^7 5d6s6p$ with 5s and 5p local orbitals; for Ti the (Ar) 3d4s4p with 3s and 3p local orbitals; for Ge the (Ar) 4s4p4d with 3p and 3d local orbitals. The $R_{mt}K_{max}$ cutoff parameter equal to 9.0 was assumed giving the basis set of 715 LAPW's. The **k**-space grid of $10 \times 10 \times 10$ was applied (99 **k**-vectors in irreducible Brillouin zone).

The valence states were treated within the scalar-relativistic approach. The gradient corrected local spin density (LSD) exchange correlation (XC) potential in the form developed by Perdew, Burke, Ernzerhof [6] (PBE) was employed. To account for the Hubbard correlation within the 4f-band states, the PBE XC potential corrected according to the LSDA+U method [7] was used for the Gd-4f states. The coulomb (U) and exchange (J) parameters, equal 6.7 and 0.7 eV, respectively, were taken from the work by Harmon et al. [8].

X-ray L_2 and L_3 absorption spectra for the Ti component atom was derived using the formalism described in Ref. [9], which employs Fermi's golden rule with dipole matrix elements between a core and conduction band state and with the partial atomic densities of states of Ti. The L_2–L_3 splitting was taken equal 5.4 eV, according to the calculated core eigenvalues. Broadening effects due to the finite life-time of the core states and the spectrometer broadening were taken into account in performing the convolution of the calculated spectra with the Lorentz functions of the half-width equal to 0.3 and 0.1 eV, respectively.

The main features of the theoretical spectrum are denoted as A, B, B^*, C, D, E, E^* and they can be compared to the experimental result. Peaks A, B, C and D can be easily ascribed to the main features of the experimental absorption spectrum. Two groups of peaks centered at about 460 and 466 eV can be related to the spin–orbit splitting of the Ti 2p level. The structure of both groups is similar indicating that mainly the density of unoccupied 3d states is responsible for this shape. The position of the peaks and distance between them allows an attribution of four peaks. The distance between the peaks A–B and C–D is 1.8 eV, whereas A–C is 5.5 eV. This value is very close to the spin–orbit splitting taken for absorption calculations. One may suppose that the structure of the unoccupied Ti 3d states is responsible for that small discrepancy. The low intensity peaks B^*, E and E^* obtained in calculations are not visible in our XAS spectrum. This may be related to their higher line-width than for other parts of the spectrum and may indicate to more delocalised final states of the absorption process. Our calculations for GdTiGe give almost no electron transfer from Ti atoms when the crystal is formed so the electronic configuration should be rather close to Ti^0. Therefore, the agreement with the atomic calculations assuming Ti^{4+} configuration is probably accidental.

Additionally, XAS and XMCD measurements have been performed for deep core levels of Gd, Ti, Ge and Si for GdTiGe and GdTiSi.

No measurable X-MCD signal is observed at the Ti K-edge (Fig. 3), which indicates a lack of polarisation of its 4p band. As the theoretical calculations indicate presence of a small magnetic moment 0.61 μ_B carried by titanium 3d electrons, the effect can be explained by a possible cancellation of the contributions to the polarisation of Ti 4p band from its own 3d moment and from a hybridisation with spin polarised Gd 5d band. An X-MCD signal has also been observed at the Ge K-edge for GdTiGe (Fig. 4). The X-MCD spectrum coincides with the rising edge of XANES spectrum. It shows a complex shape with the dominant negative peak in-between two positive peaks. This indicates existence of spin polarisation of Ge 4p electronic band arising possibly due to hybridisation with spin polarised Gd 5d band. However, calculations do not

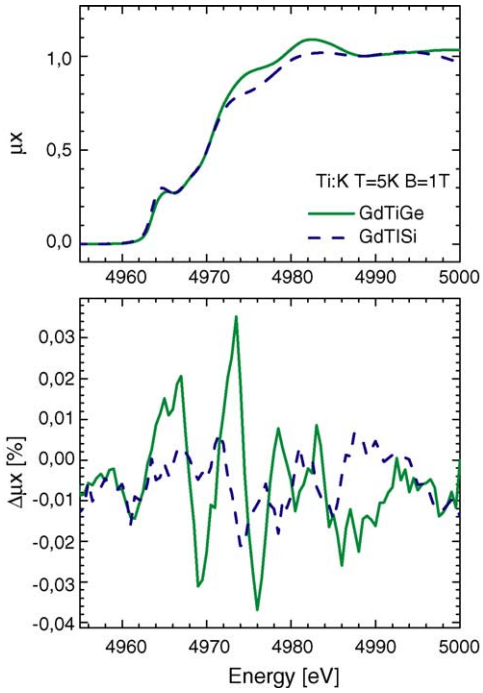

Fig. 3. Ti K-edge XAS and XMCD spectra of GdTiGe and GdTiSi.

confirm this effect (s–p polarisation is $-0.03\,\mu_B$) [1]. Gd L_2 (L_3) edge XMCD spectrum (Figs. 5 and 6) is dominated by the negative (positive) peak at the rising edge of the white line. The shape of the dichroic signal in both cases resembles the derivative of the normal (spin averaged) absorption and can be attributed to the nearly empty exchange split 5d band

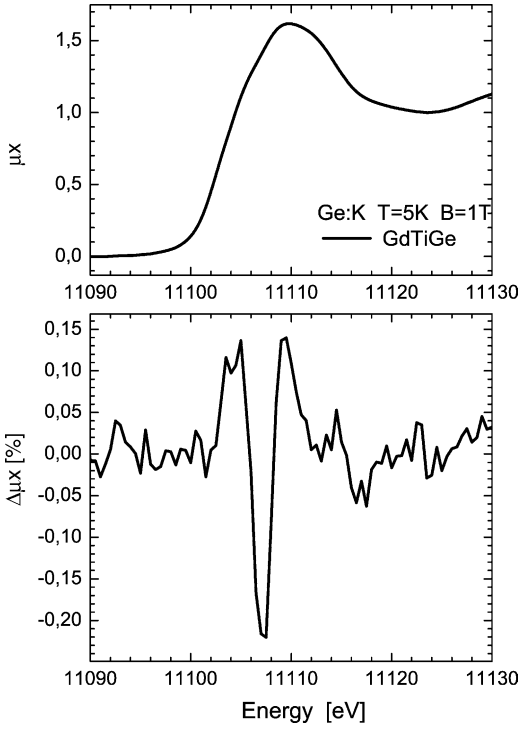

Fig. 4. Ge K-edge XAS and XMCD spectra of GdTiGe.

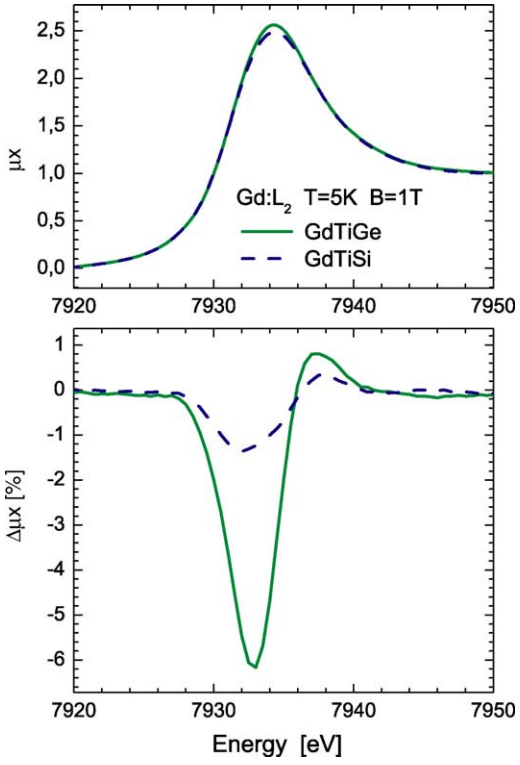

Fig. 5. Gd L_2-edge XAS and XMCD spectra of GdTiGe and GdTiSi.

which is predominantly the final state of the transitions at the Gd L_2 L_3 edges. The opposite sign of the signals at the L_2 and L_3 edges reflects the opposite senses of spin polarisation of photoelectrons at these edges. The dichroic signal

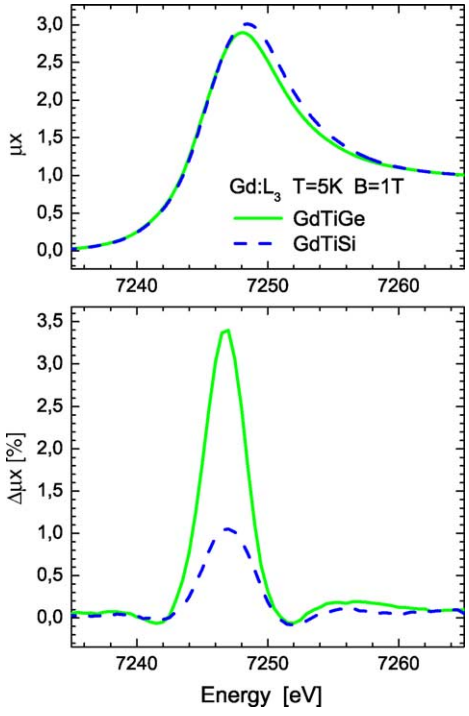

Fig. 6. Gd L_3-edge XAS and XMCD spectra of GdTiGe and GdTiSi.

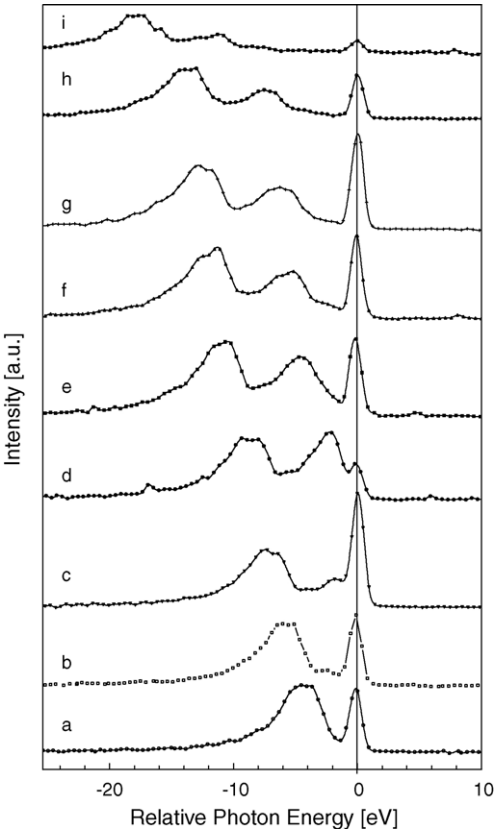

Fig. 7. RIXS spectra of GdTiGe sample at different excitation energies across the Ti $L_{2,3}$ threshold. The RIXS data are plotted against the transferred energy.

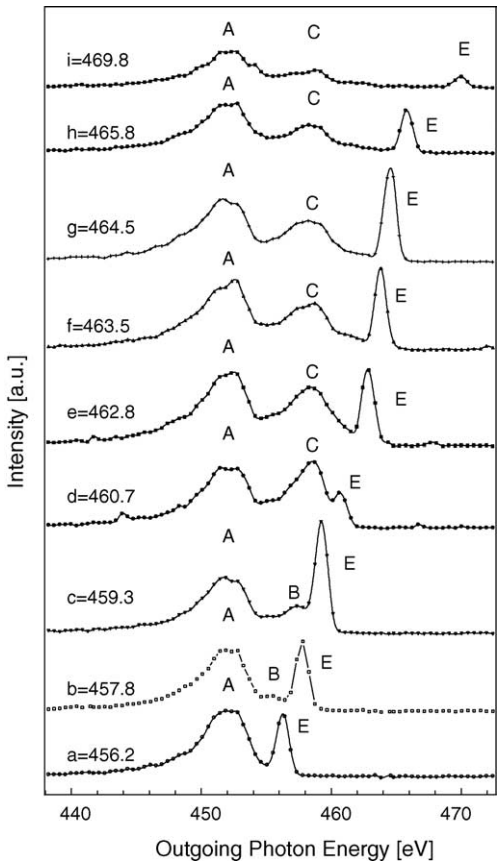

Fig. 8. RIXS spectra of GdTiGe sample at different excitation energies across the Ti $L_{2,3}$ threshold.

at the Gd L_2 L_3 edges almost five times larger in GdTiGe than GdTiSi is attributed to a much smaller magnetisation of the latter compound achieved in a 1 T field used for X-MCD measurements [1].

In RIXS, the sample is resonantly excited by a photon beam and the X-ray emission spectrum is measured. The electron is excited from a core level to unoccupied states above the Fermi level. When the process is resonant, it may be regarded as a coherent inelastic scattering process. The spectrum gives information mainly about the valence density of states. RIXS enables to obtain information about the ground state of the system via intermediate core excited states. In resonant scattering through a Ti 2p excitation, the local states of d- (and s-) symmetry at the Ti site are probed [10].

The excitation energies used in RIXS measurements are shown by vertical arrows in the XAS spectrum. The peak at zero energy loss (elastic scattering features) is visible in all spectra, allowing an accurate calibration of the energy scale (Fig. 7). The intensity of the elastic peak generally follows that of the XAS spectrum and can be attributed directly to the density of unoccupied Ti states. One can also observe normal emission (fluorescence) features at constant photon emission energy (Fig. 8). The one at the energy range 451–453 eV is visible for all excitation energies used and the second one appears at about 459 eV for excitations above 460 eV. The first one can be ascribed to the $3d–2p_{3/2}$ transitions, whereas the second one comes from the transitions to the $2p_{1/2}$ level. The shape of the peaks can be compared to the XPS valence band spectra and partial densities of Ti 3d states [1] obtained using calculations. It is in good agreement with the XPS measurements. One can see that line A is split in two smaller peaks, which are visible also in the calculated DOS. Due to the relatively large line broadening in RIXS this structure is only slightly manifested but we suppose it can be related to two distinct peaks in partial Ti DOS situated at binding energy of 1–2 eV [1]. Changes of the relative intensity of two structures visible within peak A ($3d–2p_{3/2}$) are connected with excitation energy. When the energy is tuned to values which are close to the first peaks in the spin–orbit split absorption spectrum (b, e and f) one observes an enhancement of the emission from the higher energy part of the band A. The opposite situation (enhancement of lower energy emission part) can be noticed for excitation energies c and g just at the maxima of absorption of L_2 and L_3 edges. The variation of intensity can be then explained by a resonant enhancement of the emission from the occupied Ti 3d bands when electrons are excited to unoccupied states with the same orbital character and at the same **k**-vector in the Brillouin zone.

Some resonating inelastic scattering features appear also at energies 2–3 eV below the excitation energy. Inelastic

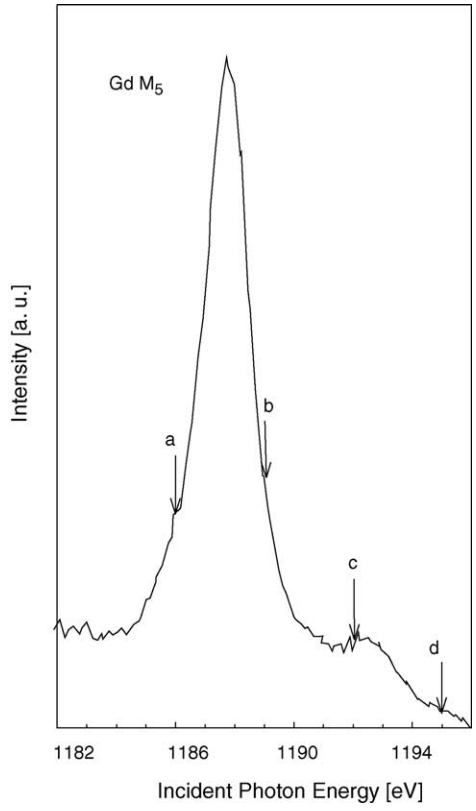

Fig. 9. Gd M_5-edge XAS spectrum of GdTiGe.

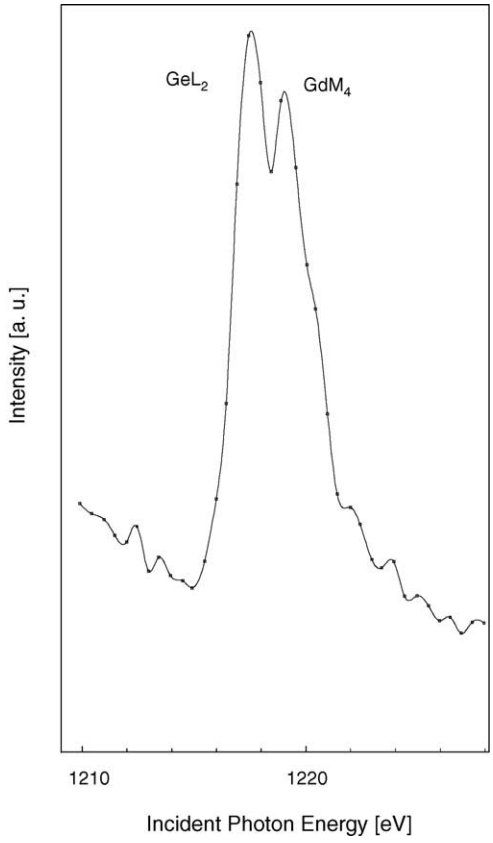

Fig. 10. Gd M_4 and Ge L_2-edge XAS spectrum of GdTiGe.

emission structures are observed for excitation energies corresponding to both peaks in the absorption spectra—457.8 and 459.3 eV. It can be related to resonant intraband excitations in the 3d bands, similarly to those mentioned by Uehara et al. [11]. One can also observe the changes in relative intensity ratio between the fluorescence related to transitions to the Ti $2p_{1/2}$ and $2p_{3/2}$ levels.

The XAS spectrum at Gd M_4 and M_5 edges have been obtained at room temperature at ELETTRA (Figs. 9 and 10). The spectrum contains also a line from the Ge L_3 edge absorption visible at energy of about 1217 eV. The second line can be attributed to Gd M_4 edge. It is worth noting that the observed structure is similar to the one found in the XPS spectrum which will be published elsewhere.

The Gd M_5 edge shows a shape, which enables to distinguish few structures: a bump at 1186 eV, the main peak at 1187.8 eV and second peak at 1192.3 eV. This structure can be compared to the earlier results obtained for Gd metal [12] and $Gd_3Ga_5O_{12}$ [13]. There are no significant differences between the spectrum obtained for GdTiGe and the mentioned materials except the different energy position of the main peak. Calculations using the LAPW method (Fig. 11) give a main peak which is related to the $3d^94f^8$ configuration and some structure at higher energy which, however, has much less intensity than in the experimental spectrum.

We measured also RIXS spectrum at the photon energies in the vicinity of Gd M_5 absorption edge (Fig. 12). A

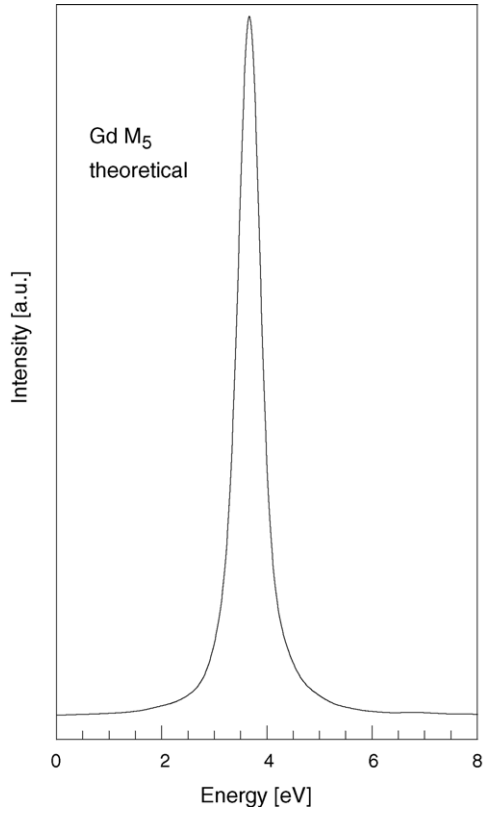

Fig. 11. Calculated Gd M_5-edge XAS spectrum of GdTiGe.

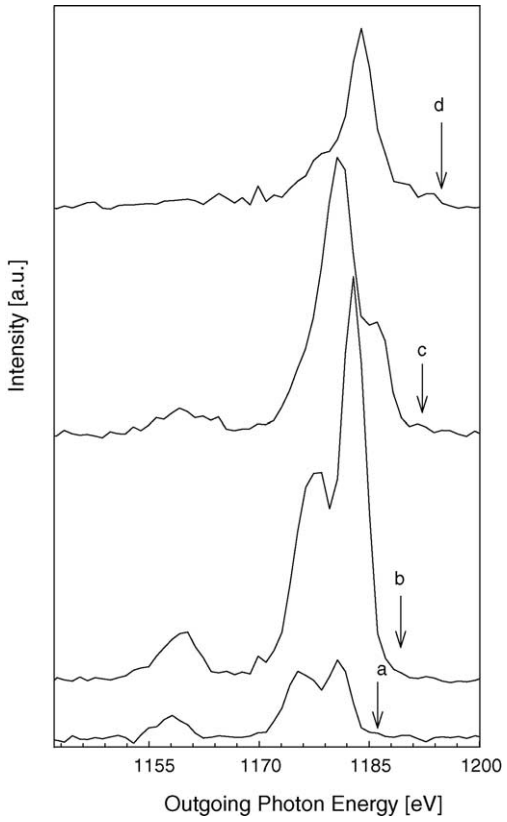

Fig. 12. RIXS spectra of GdTiGe sample at different excitation energies across the Gd M_5 threshold.

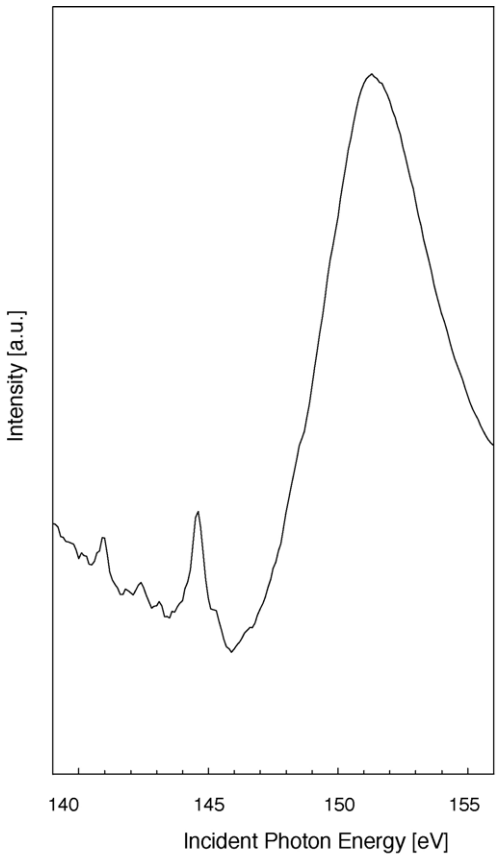

Fig. 13. Gd $N_{4,5}$-edge XAS spectrum of GdTiGe.

characteristic feature of the obtained spectra is the lack of elastic peak and strong variation of the emission with the photon energy. For each energy, one can observe a double peak structure with the distance between peaks of the order of 5–7 eV.

The unoccupied 4f states are characterized by the spin direction, which is opposite to the ground state of the 4f level. Electronic transitions, which are responsible for the emission in the energy range 1174–1184 eV are mainly due to the $3d^9 4f^8$ excited state. The relative spin direction of the ground, excited and final states are important. The detailed analysis of the intermediate state $3d^9 4f^8$ structure and consequent 4f–3d transitions is beyond the frames of this article. However, one can suppose that the structure of the exchange split $3d_{5/2}$ level is also responsible for the observed features and relative intensity changes. The XPS data show that this level is obviously broadened due to the exchange splitting (FWHM about 6 eV) although the particular lines cannot be distinguished. The discussed X-ray emission structure is much different from the one described by Dallera et al. for $Gd_3Ga_5O_{12}$ [13]. This means that not only atomic effects should be taken into account but also the influence of the band structure is important. On the other hand, the XAS Gd $N_{4,5}$ spectrum obtained at room temperature has shown the same structure as reported in the earlier results for Gd metal (Fig. 13). This spectrum is formed by the 4d–4f transitions with clearly visible pre-peaks at energies of about 138–145 eV [14].

To understand the origin of the observed emission spectra further theoretical calculations are necessary which will take into account the possible matrix elements and the band structure.

4. Conclusions

We have reported the results of investigation of electronic structure obtained with XAS, XMCD and RIXS techniques for GdTiGe and partly for GdTiSi. Low temperature, high field XMCD shows for GdTiGe a significant Gd 5d electron polarisation and small one for Ge 4p states. Ti $L_{2,3}$ absorption spectrum is close to the model one obtained using LAPW calculations. The resonant structures in RIXS have been observed for excitations energies close to the Ti $2p_{3/2}$ thresholds for GdTiGe. They can be related to the Ti 3d intraband transitions. The observed variation of relative intensities within the emission spectra can be explained by a resonant enhancement of the emission related to transitions from the occupied Ti 3d bands X-ray emission obtained for Gd M_5 edge shows a complex behaviour and requires further experimental and theoretical studies. It shows different behaviour to reported earlier results for the Gd oxidic compound.

Acknowledgments

This work was supported by European Community under project HPRI-CT-1999-00033. Partial support of the State Committee for Scientific Research, Poland is acknowledged.

References

[1] G. Skorek, J. Deniszczyk, J. Szade, B. Tyszka, J. Phys. Condens. Matter 13 (2001) 6397.
[2] F.M.F. de Groot, J.C. Fuggle, Phys. Rev. B 42 (1990) 5459.
[3] F.M.F. de Groot, J.C. Fuggle, Phys. Rev. B 41 (1990) 928.
[4] M. Stener, G. Fronzoni, M. De Simone, Chem. Phys. Lett. 373 (2003) 115.
[5] P. Blaha, K. Schwarz, G.K.H. Madsen, D. Kvasnicka, J. Luitz, WIEN2k, An Augmented Plane Wave + Local Orbitals Program for Calculating Crystal Properties, Karlheinz Schwarz, Techn. Universität Wien, Austria, 2001, ISBN 3-9501031-1-2.
[6] J.P. Perdew, K. Burke, M. Ernzerhof, Phys. Rev. Lett. 77 (1996) 3865.
[7] V.I. Anisimov, J. Zaanen, O.K. Andersen, Phys. Rev. B 44 (1991) 943.
[8] B.N. Harmon, V.P. Antropov, A.I. Lichtenstein, I.V. Solovyev, V.I. Anisimov, J. Phys. Chem. Solids 56 (1995) 1521.
[9] A. Neckel, K. Schwarz, R. Eibler, P. Rastl, Microchim. Acta 257 (Suppl. 6) (1975);
K. Schwarz, E. Wimmer, J. Phys. F Met. Phys. 10 (1980) 1001.
[10] A. Augustsson, A. Hennigsson, S.M. Butorin, H. Siegbahn, J. Nordgren, J.H. Guo, J. Chem. Phys. 119 (2003) 3983.
[11] Y. Uehara, D.W. Lindle, T.A. Callcott, L.T. Terminello, F.J. Himpsel, D.L. Ederer, J.H. Underwood, E.M. Gullikson, R.C.C. Perera, Appl. Phys. A 65 (1997) 179.
[12] M. Taguchi, L. Braicovich, G. Ghiringhelli, A. Tagliaferri, F. Borgatti, C. Dallera, K. Giarda, N.B. Brookes, Phys. Rev. B 63 (2001) 235113.
[13] C. Dallera, L. Braicovich, G. Ghiringhelli, M.A. van Veenendaal, J.B. Goedkoop, N.B. Brookes, Phys. Rev. B 56 (1997) 1279.
[14] K. Starke, E. Navas, E. Arenholz, Z. Hu, L. Baumgarten, G. Van der Laan, C.T. Chen, G. Kaindl, Phys. Rev. B 55 (1997) 2672.